Catalytic Hydrogenation of Diphenylacetylene by a Layer-Segregated Platinum–Ruthenium Cluster Complex

Richard D. Adams,* Thomas S. Barnard, Zhaoyang Li, Wengan Wu, and John H. Yamamoto

Contribution from the Department of Chemistry and Biochemistry, University of South Carolina, Columbia, South Carolina 29208

*Received May 13, 1994**

Abstract: The complex $Pt_3Ru_6(CO)_{20}(\mu_3\text{-}PhC_2Ph)(\mu_3\text{-}H)(\mu\text{-}H)$ (**1a**) has been found to be an effective catalyst for the hydrogenation of diphenylacetylene to (*Z*)-stilbene at 50 °C and 1 atm of hydrogen. The turnover frequency (TOF) of 47(1) h^{-1} was observed at a catalyst concentration of 10^{-4} M and alkyne concentration of 10^{-2} M. Kinetic studies of this reaction have revealed the rate expression, $R = k[\mathbf{1a}][PhC_2Ph]p(H_2)/p(CO)(1 + k'[PhC_2Ph])$. Measurement of the rates as a function of temperature has allowed determination of the activation parameters, $\Delta H^* = 24.9(6)$ kcal/mol and $\Delta S^* = 1.4(9)$ eu. The complex $Pt_3Ru_6(CO)_{20}(\mu_3\text{-}TolC_2Tol)(\mu_3\text{-}H)(\mu\text{-}H)(\mu\text{-}H)$ (**1b**) was also prepared. The TOF for the hydrogenation of $TolC_2Tol$ to (*Z*)-Tol(H)C=C(H)Tol by **1b** is 30(1) h^{-1}. At high alkyne/**1a** ratios (1000/1), side reactions become important after a few hundred turnovers and the catalyst is transformed into species that have low catalytic activity. Four of these complexes have been isolated and characterized. Three of these are the new complexes $Ru_6Pt_3(CO)_{18}(\mu_3\text{-}\eta^6\text{-}PhC_2H_4Ph)(\mu_3\text{-}H)_4$ (**2a**), $Ru_6Pt_3(CO)_{18}(\eta^6\text{-}PhCH_2CH_2Ph)(\mu_3\text{-}H)_4$ (**3a**), and $Ru_6Pt_3(CO)_{15}(\mu_3\text{-}PhC_2Ph)_3(\mu\text{-}H)_6$ (**4**), and one is the previously reported compound $Ru_6Pt_3(CO)_{14}(\mu_3\text{-}Ph_2C_2)_3$ (**5**). The tolyl analog of **3a**, $Ru_6Pt_3(CO)_{18}(\eta^6\text{-}TolCH_2CH_2Tol)(\mu_3\text{-}H)_4$ (**3b**), was also prepared. Complexes **2a**, **3b**, and **4** were characterized by single crystal X-ray crystallographic analyses. The molecular structures of **2a** and **3b** were found to consist of three triangular groups of three metal atoms arranged in a face-shared bioctahedral structure. The central triangle is pure platinum and the outer triangles are pure ruthenium as also found in the compound **1a**. Both compounds contain diarylethane ligands which are π-coordinated to the cluster through one of the aryl rings. In **2a**, the coordinated ring is bridging three metal atoms, while in **3b**, it is coordinated to only one metal atom. Compounds **3a,b** are believed to be isostructural. The structure of **4** consists of a raftlike structure of three ruthenium and three platinum atoms. The central triangular group contains the three platinum atoms. The three remaining ruthenium atoms bridge Ru–Pt edges of the raft, and all three lie on one side of the Pt_3Ru_3 plane producing an overall C_3 symmetry of the cluster. Each of the three Ru_2Pt triangles contains a triply bridging PhC_2Ph ligand and one edge bridging hydride ligand. The remaining three hydride ligands bridge Pt–Ru edges of the Pt_3Ru_3 raft. The catalytic activity of a variety of related platinum and ruthenium complexes toward hydrogenation of PhC_2Ph was tested under conditions identical to those used for **1a,b**, but none are as active as compounds **1a,b**. A mechanism for the catalysis based on complex **1a** is proposed that begins with dissociation of a CO ligand from the cluster. This is followed by hydrogen activation and alkyne addition steps. The latter is believed to induce the transfer of the hydride ligands to the coordinated alkyne in the slow step of the reaction. It is suggested that the unusually high activity of the catalysis is produced in part by a synergistic interplay of the small molecule activations occurring at the platinum and ruthenium layers of the metal. Crystal data. For **2a**: space group = $P2_1/n$, $a = 16.648(3)$ Å, $b = 14.065(3)$ Å, $c = 17.558(3)$ Å, $\beta = 92.78(1)°$, $Z = 4$, 2625 reflections, $R = 0.033$. For **3b**: space group = $P2_1/n$, $a = 17.192(3)$ Å, $b = 12.126(3)$ Å, $c = 22.649(4)$ Å, $\beta = 111.98(1)°$, $Z = 4$, 3023 reflections, $R = 0.030$. For **4**: space group = $P2_1/n$, $a = 13.567(2)$ Å, $b = 36.282(9)$ Å, $c = 13.711(2)$ Å, $Z = 4$, 4178 reflections, $R = 0.049$.

Introduction

It is well-known that metal alloys can exhibit catalytic properties that can be vastly different from and in some cases superior to those of the pure metals.[1] It has been suggested that some of the unique properties of alloy catalysts can be attributed to different steps of the reaction occurring cooperatively at the different types of metal atoms.[2] Recent studies have indicated that metal cluster complexes are capable of performing a variety of organic reactions catalytically,[3] and there is evidence that some mixed metal complexes may also possess reactivity properties due to cooperative interactions between the different types of metal atoms.[4] The term "synergism" has been used to describe these effects.[5] Synergism is also expressed by bimetallic heterogeneous catalysts.

We have recently prepared the layer segregated metal cluster complex $Pt_3Ru_6(CO)_{20}(\mu_3\text{-}PhC_2Ph)(\mu_3\text{-}H)(\mu\text{-}H)$ (**1a**). This compound contains three triangular layers of three metal atoms. The

* Abstract published in *Advance ACS Abstracts*, September 1, 1994.

(1) (a) Sinfelt, J. H. *Bimetallic Catalysts. Discoveries, Concepts and Applications*; Wiley: New York, 1983. (b) Sinfelt, J. H. *Sci. Am.* **1985**, *253*, 90. (c) Sinfelt, J. H. *Acc. Chem. Res.* **1977**, *10*, 15. (d) Sachtler, W. M. H. *J. Mol. Catal.* **1984**, *25*, 1. (e) Guczi, L. *J. Mol. Catal.* **1984**, *25*, 13. (f) Sachtler, W. M. H.; van Santen, R. A. *Adv. Catal.* **1977**, *26*, 69. (g) Ponec, V. *Adv. Catal.* **1983**, *32*, 149. (h) Biswas, J.; Bickle, G. M.; Gray, P. G.; Do, D. D.; Barbier, J. *Catal. Rev.—Sci. Eng.* **1988**, *30*, 161. (i) Diaz, G.; Garin, F.; Maire, G. *J. Catal.* **1983**, *82*, 13. (j) Braunstein, P.; Devenish, R.; Gallezot, P.; Heaton, B. T.; Humphreys, C. J.; Kervennal, J.; Mulley, S.; Ries, M. *Angew. Chem., Int. Ed. Engl.* **1988**, *27*, 927.

(2) Goodman, D. W.; Houston, J. E. *Science* **1987**, *236*, 403.

(3) (a) Süss-Fink, G.; Meister, G. *Adv. Organomet. Chem.* **1993**, *35*, 41. (b) Süss-Fink, G.; Neumann, F. In *The Chemistry of the Metal-Carbon Bond*; Hartley, F. R., Ed.; Wiley: Chichester, England, 1989; Vol. 5, p 231. (c) Gates, B. C., Guczi, L., Knözinger, H., Eds. *Metal Clusters in Catalysis*; Elsevier: Amsterdam, The Netherlands, 1986. (d) Gladfelter, W.; Roesselet, K. J. In *The Chemistry of Metal Cluster Complexes*; Shriver, D., Kaesz, H. D., Adams, R. D., Eds.; VCH: Weinheim, Germany, 1990; Chapter 7, p 329. (e) Castiglioni, M.; Giordano, R.; Sappa, E. *J. Organomet. Chem.* **1989**, *369*, 419. (f) Castiglioni, M.; Giordano, R.; Sappa, E. *J. Organomet. Chem.* **1989**, *362*, 399.

(4) (a) Braunstein, P.; Rosé, J. In *Stereochemistry of Organometallic and Inorganic Compounds*; Bernal, I., Ed.; Elsevier: Amsterdam, 1989; Vol. 3. (b) Giordano, R.; Sappa, E. *J. Organomet. Chem.* **1993**, *448*, 157. (c) Adams, R. D.; Babin, J. E.; Tasi, M.; Wang, J.-G. *Organometallics* **1988**, *7*, 755. (d) Castiglioni, M.; Giordano, R.; Sappa, E. *J. Organomet. Chem.* **1988**, *342*, 111. (e) Castiglioni, M.; Giordano, R.; Sappa, E. *J. Organomet. Chem.* **1987**, *319*, 167. (f) Ojima, I.; Donovan, R. J.; Ingallina, P.; Clos, N.; Shay, W. R.; Eguchi, M.; Zeng, Q.; Korda, A. *J. Cluster Sci.* **1992**, *3*, 423.

(5) (a) Golodov, V. A. *J. Res. Inst. Catal., Hokkaido Univ.* **1981**, *29*, 49. (b) Dombek, B. D. *Organometallics* **1985**, *4*, 1707.

0002-7863/94/1516-9103$04.50/0

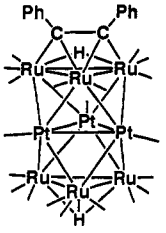

1a

central layer consists of pure platinum while the outer layers are pure ruthenium. The PhC_2Ph ligand is a triple bridge on one of the triruthenium triangles.[6] Compound **1a** adds CO in the presence of a CO atmosphere, and the hydride ligands are sequentially transferred to the PhC_2Ph ligand to form (*Z*)-stilbene, Ph(H)C=C(H)Ph, which is released from the complex.[6a] We have now found that **1a** reacts with hydrogen in the presence of free PhC_2Ph to produce (*Z*)-stilbene catalytically at an unusually high rate (47(1) turnovers/(mol·h) at 50 °C and 1 atm of H_2) for a cluster compound. The results of this study are reported here. A preliminary report of this work has been published.[6b]

Experimental Section

General Procedures. All the reactions were performed under an atmosphere of nitrogen unless otherwise indicated. Reagent grade solvents were dried over sodium and deoxygenated by purging with N_2 prior to use. Except for purging with nitrogen prior to use, reagent grade CH_2Cl_2 was used as purchased and was not subjected to rigorous drying. $Pt_3Ru_6(CO)_{20}(\mu_3\text{-}PhC_2Ph)(\mu_3\text{-}H)(\mu\text{-}H)$[6] (**1a**), $Pt(PhC_2Ph)_2$,[7] $Ru(CO)_5$,[8] $Ru_3(CO)_9(Ph_2C_2)(\mu\text{-}H)_2$,[9] $Ru_3(CO)_9(\mu_3\text{-ampy})(\mu\text{-}H)$,[10] and $PtRu_2(CO)_8(PhC_2Ph)(dppe)$[11] were prepared by previously reported procedures. $Ru_3(CO)_{12}$ was purchased from Strem Chemicals, Inc., and was recrystallized before use. Diphenylacetylene and di-*p*-tolylacetylene ($TolC_2Tol$) were purchased from Aldrich and were purified by column chromatography. Hydrogen (SUNOX, Inc.) and deuterium (Union Carbide Corp., Linde Division) were used without further purification. IR spectra were recorded on a Nicolet 5DXB FT-IR spectrophotometer. ^1H NMR spectra were recorded on a Bruker AM-300 FT-NMR spectrometer. Elemental microanalyses were performed by Desert Analytics, Tucson, AZ. TLC separations were performed in air by using silica gel (60 Å, F_{254}) on plates (Whatman, 0.25 mm). GLC analyses were made by using a Perkin-Elmer Sigma 300 chromatograph with a flame ionization detector and a EconoCap SE-30 column (Alltech 2096-14, 0.25 mm, 30 m). Calibrations were made using standard samples. Reaction rates were obtained by measuring the PhC_2Ph consumption as a function of time. Plots of the kinetic data were fitted using Cricket Graph version 1.3 of Cricket Software on a Macintosh LCII personal computer.

Preparation of $Ru_6Pt_3(CO)_{20}(\mu_3\text{-}TolC_2Tol)(\mu_3\text{-}H)(\mu\text{-}H)$ (1b). This compound was prepared according to the same procedure that was used to prepare **1a** with the substitution of $TolC_2Tol$ for PhC_2Ph.[6] IR (ν(CO) in CH_2Cl_2): 2097 (w), 2067 (s), 2047 (m), 2033 (m). ^1H NMR for **1b** (δ in CD_2Cl_2 at −90 °C): 6.99 (d, 4H, J_{H-H} = 8.3 Hz), 6.95 (d, 4H, J_{H-H} = 8.3 Hz), 2.23 (s, 6H), −18.02 (s, 1H), −18.75 (s, 1H).

General Procedures for the Kinetic Studies. All catalytic studies were conducted in a solvent mixture of CH_2Cl_2 and hexane in a 3/49 v/v ratio. The appropriate amounts of catalyst and PhC_2Ph and a stir bar were placed in a three-necked flask (50 or 25 mL) with one neck connected to a vacuum line and nitrogen inlet through a stopcock, another connected to a water-cooled condensor, and the third closed with a rubber septum.

Table 1. Turnover Frequency (TOF) for Formation of (*Z*)-Stilbene

time (h)	TOF (h^{-1})
1	80.2
2	82.4
3	64.0
4	45.2
5	40.6
6	41.6
7	38.0
8	29.9
9	16.3
10	19.8
11	12.5
12	8.5
13	6.0
total time: 13 h	total turnovers: 493

The system was evacuated and filled with nitrogen five times. The appropriate amount of CH_2Cl_2 was placed in the flask via syringe and allowed to stir at room temperature for 10 min to dissolve the catalyst completely. Then the appropriate amount of hexane was introduced via syringe, and the system was purged with hydrogen at room temperature for 5 min. The flask was then immersed in a thermostated bath at 323 K, and hydrogen was purged slowly through the solution. After the reaction was stopped, the solvent was removed under reduced pressure and the residues were separated by TLC. All the kinetic experiments were performed at least twice. Except for the alkyne dependence measurements, in all cases, the reaction rates per hour were determined by measuring either the amount of PhC_2Ph consumed or the amount of (*Z*)-stilbene formed after a period of *1* h as established by separation of the components from an aliquot of the reaction solution by gas chromatography.

Hydrogenation of PhC_2Ph by 1a at a 100/1 PhC_2Ph/1a Ratio. A 10.0-mg amount of **1a** (0.005 18 mmol) and 92.0 mg of PhC_2Ph (0.518 mmol) were dissolved in 3.0 mL of CH_2Cl_2, and 49.0 mL of hexane was then added to bring the total to 52.0 mL (10^{-4} M in catalyst). The experiment was carried out under the conditions described. After 1 h, 47% of the PhC_2Ph was converted to (*Z*)-stilbene.[12] After 3 h, the reaction was terminated. GLC showed that 81% of the PhC_2Ph was converted to (*Z*)-stilbene and 4% to (*E*)-stilbene. There was trace of 1,2-diphenylethane (bibenzyl), and 15% of the PhC_2Ph was recovered. Separation of the complexes by TLC yielded 4.9 mg of **1a**, a trace amount of the known compound $Ru_6Pt_3(CO)_{14}(\mu_3\text{-}PhC_2Ph)_3$,[11] and 1.8 mg of a mixture of the two isomers $Ru_6Pt_3(CO)_{18}(\mu_3\text{-}\eta^6\text{-}PhC_2H_4Ph)(\mu\text{-}H)_4$ (**2a**) and $Ru_6Pt_3(CO)_{18}(\eta^6\text{-}PhCH_2CH_2Ph)(\mu_3\text{-}H)_4$ (**3a**) (combined yield 18%). Compounds **2a** and **3a** can be separated by repeated applications of TLC. Compound **2a** elutes faster than **3a**. Note that **2a** also slowly isomerizes to **3a** over a period of time, see details below. Spectra for **2a**. IR (ν(CO) in hexane): 2090 (m), 2050 (vs), 2040 (sh, s), 2022 (sh, m), 2020 (sh, m), 2001 (w). ^1H NMR (δ in CD_2Cl_2 at 25 °C): 7.25–7.50 (m, 5H), 4.61 (t, br, 1H), 4.26–4.26 (m, 4H), 3.16 (t, 2H, $^3J_{H-H}$ = 7.0 Hz), 2.83 (t, 2H, $^3J_{H-H}$ = 7.0 Hz), −16.18 (s, br, 4H, $\Delta\nu_{1/2}$ = 370 Hz). Spectra for **3a**. IR (ν(CO) in CH_2Cl_2): 2088 (m), 2046 (vs), 2020 (m). ^1H NMR (δ in CD_2Cl_2 at 25 °C): 7.29 (t, 2H, J_{H-H} = 7.2 Hz), 7.24 (d, 1H, J_{H-H} = 7.2 Hz), 7.10 (d, 2H, J_{H-H} = 7.2 Hz), 5.98 (t, 2H, J_{H-H} = 5.7 Hz), 5.83 (t, 1H, J_{H-H} = 5.7 Hz), 5.90 (d, 2H, J_{H-H} = 5.7 Hz), 2.96 (t, 2H, $^3J_{H-H}$ = 7.3 Hz), 2.72 (t, 2H, $^3J_{H-H}$ = 7.3 Hz), −15.34 (t, 4H, J_{Pt-H} = 77 Hz; J_{Pt-H} = 26 Hz). There was no detectable difference in the rates of formation of (*Z*)-stilbene between reactions performed in the dark and those performed in the usual lighting of the laboratory.

Catalytic Hydrogenation of PhC_2Ph by 1a at a 1000/1 PhC_2Ph/1a Ratio. A 920.0-mg amount (5.18 mmol) of PhC_2Ph and 10.0 mg (0.005 18 mmol) of **1a** were dissolved in a mixture of 3.0 mL of CH_2Cl_2 and 49.0 mL of hexane. The other conditions were as previously described. The formation of (*Z*)-stilbene was followed by GLC at hourly intervals for 13 h. The turnover rates as a function of time are listed in Table 1.

At the end of the period, the organic compounds were removed by column chromatography and the metal complexes were separated by TLC using a hexane/CH_2Cl_2 (3/1) solvent mixture. This yielded 0.9 mg of **1a**, 2.5 mg of the new compound $Ru_6Pt_3(CO)_{15}(\mu_3\text{-}PhC_2Ph)_3(\mu\text{-}H)_6$ (**4**), 1.7 mg of $Ru_6Pt_3(CO)_{14}(\mu_3\text{-}PhC_2Ph)_3$[11] (**5**), and 1.1 mg of a mixture of **2a** and **3a**. Spectra for **4**. IR (ν(CO) in hexane): 2098 (m), 2086 (m),

(6) (a) Adams, R. D.; Li, Z.; Wu, W.; Yamamoto, J. *Organometallics* **1994**, *13*, 2357. (b) Adams, R. D.; Li, Z.; Wu, W.; Swepston, P.; Yamamoto, J. *J. Am. Chem. Soc.* **1992**, *114*, 10657.
(7) Boag, N. M.; Green, M.; Grove, M. D.; Howard, J. A. K.; Spencer, J. L.; Stone, F. G. A. *J. Chem. Soc., Dalton Trans.* **1980**, 2170.
(8) Huq, R.; Poë, A. J.; Chawla, S. *Inorg. Chem. Acta* **1980**, *38*, 121.
(9) (a) Giordano, R.; Sappa, E. *J. Organomet. Chem.* **1993**, *448*, 157. (b) Castiglioni, M.; Giordano, R.; Sappa, E. *J. Organomet. Chem.* **1983**, *258*, 217. (c) Sappa, E.; Gamblino, O.; Cetini, G. *J. Organomet. Chem.* **1972**, *44*, 185.
(10) Cabeza, J. A.; Fernandez-Colinas, J. M.; Llamazares, A.; Riera, V. *J. Mol. Catal.* **1972**, *71*, L7–L11.
(11) Adams, R. D.; Wu, W. *Organometallics* **1992**, *12*, 1248.
(12) Pouchert, C. J. *Aldrich Library of NMR Spectra*, 2nd ed.; 1983; Vol. 1, p 1752.

Table 2

concn of PhC_2Ph (M)	reaction rate (M/min)
0.0100	0.000 091 3
0.0150	0.000 103
0.0250	0.000 116
0.0500	0.000 128
0.0750	0.000 133
0.1000	0.000 134

Table 3

amt of cat (mg)	Cat concn (mM)	k_{obs} (min^{-1})
2.5	0.0250	0.002 39
5.0	0.0500	0.004 88
7.5	0.0750	0.008 09
10.0	0.100	0.010 4
12.5	0.125	0.012 6
15.0	0.150	0.014 9

2048 (vw), 2037 (vs), 2027 (w), 2010 (m), 1994 (m). ^1H NMR (δ in CD_2Cl_2 at −73 °C): 7.22–7.24 (m, 30 H), −8.59 (s, 3H), −16.01 (s, 3H). The hydride resonances were not observed at 25 °C. Anal. Calcd (found): C, 33.80% (34.16%); H, 2.23% (2.19%).

Hydrogenation of $TolC_2Tol$ by 1b. A 5.1-mg amount of **1b** (0.0026 mmol) and a 53.3-mg amount of $TolC_2Tol$ (0.258 mmol) were dissolved in 1.5 mL of CH_2Cl_2 and 24.5 mL of hexane. The reaction was performed under the standard conditions and followed for 2 h. After 1 h, 30% of the $TolC_2Tol$ had been transformed to (*Z*)-Tol(H)C=C(H)Tol. The TOF for the formation of (*Z*)-Tol(H)C=C(H)Tol is thus 30 h^{-1}. No (*E*)-Tol(H)C=C(H)Tol was detected in this reaction. Separation of the complexes by TLC (hexane/CH_2Cl_2 = 2/1) after 2 h yielded 3.8 mg of **1b** and 0.5 mg of $Ru_6Pt_3(CO)_{18}(\eta^6\text{-}TolCH_2CH_2Tol)(\mu\text{-}H)_4$ (**3b**) (10% yield).

Procedure for the Preparation of $Ru_6Pt_3(CO)_{18}(\eta^6\text{-}TolCH_2CH_2Tol)(\mu_3\text{-}H)_4$ (3b). A 10.0-mg amount of **1b** (0.005 10 mmol) and a 31.5-mg amount of $TolC_2Tol$ (0.153 mmol) were dissolved in 30 mL of hexane in a three-necked 50-mL flask with a magnetic stir bar. The flask was purged with hydrogen and then heated to 50 °C with a thermostated oil bath. After 1.5 h, the solvent was removed and the residue was separated by TLC (hexane/CH_2Cl_2 (4/1)) to yield 5.0 mg of unreacted **1b** and 2.1 mg of $Ru_6Pt_3(CO)_{18}(\eta^6\text{-}TolCH_2CH_2Tol)(\mu\text{-}H)_4$ (**3b**) (21%). Spectra for **3b**. IR (ν(CO) in CH_2Cl_2): 2089 (m), 2050 (vs), 2043 (sh, s), 2017 (w), 1993 (vw). ^1H NMR (δ in CD_2Cl_2 at 25 °C): 7.95–7.09 (dd, 4H), 5.87–6.05 (dd, 4H), 2.92 (t, 2H, $^3J_{H-H}$ = 7.1 Hz), 2.62 (t, 2H, $^3J_{H-H}$ = 7.1 Hz), 2.31 (s, 3H), 2.24 (s, 3H), −14.70 (t, 4H, J_{Pt-H} = 100 Hz). At −88 °C, two hydride resonances were observed at −13.52 (s, 3H), and −18.18 (s, 1H). Anal. Calcd (found): C, 21.38% (21.75%); H, 1.15% (1.09%).

Kinetic Studies. Dependence of Reaction Rate upon Alkyne Concentration. A 5.0-mg or 10.0-mg amount of **1a** and an appropriate amount of PhC_2Ph were dissolved in 1.5 mL of CH_2Cl_2 and 24.5 mL of hexane or 3.0 mL of CH_2Cl_2 and 49.0 mL of hexane, respectively. The hydrogenation reactions were performed under standard conditions. The rate determinations were made by measuring the amount of (*Z*)-stilbene at the end of the first 30 min of reaction time in each case. The results are listed in Table 2.

Dependence upon Catalyst Concentration. PhC_2Ph (92.0 mg, 0.518 mmol) and the appropriate amount of catalyst (**1a**) were dissolved in 3.0 mL of CH_2Cl_2, then 49.0 mL of hexane was added. The PhC_2Ph concentration was thus 10^{-2} M in all trials. Other aspects of the hydrogenation were performed under the unusual conditions. The observed rate constants k_{obs} were obtained by measuring the consumption of alkyne as a function of time. The results are listed in Table 3.

Hydrogen Dependence Measurements. A 5.0-mg amount of **1a** (0.002 59 mmol), a 46.0-mg amount of PhC_2Ph (0.259 mmol), and a stir bar were placed in a three-necked 50-mL flask. One neck was connected to a gas buret filled with mercury and a manometer and was connected to a vacuum line. Another neck of the flask was connected to the hydrogen tank, and the third neck was sealed with a rubber septum. A 1.5-mL portion of CH_2Cl_2 was introduced into the flask by syringe through the rubber septem to dissolve the catalyst, then 24.5 mL of hexane was similarly introduced. The system was evacuated and filled with hydrogen seven times to 1 atm. The pressure was then reduced to the desired pressure, and the flask was immersed in an oil bath thermostated at 323 K. A constant hydrogen pressure was maintained by adjusting the level of the mercury in the gas buret during the course of the reaction. An equilibration time of 5 min was allowed before taking measurements. The partial pressure of hydrogen was determined by subtracting the solvent vapor pressure (premeasured) from the total pressure. Each reaction was allowed to proceed for 1 h only. The formation of (*Z*)-stilbene was determined by GLC. The results are listed in Table 4.

Table 4. Turnovers of (*Z*)-Stilbene as a Function of Hydrogen Pressure

H_2 pressure (atm)	no. of turnovers/h
0.1	5.83
0.2	10.49
0.3	15.03
0.4	21.37
0.5	27.14

Table 5. Effects of CO on TOF for Hydrogenation of PhC_2Ph by **1a**

CO fraction	1/*p*(CO)	TOF
0.05	20	3.0
0.075	13.3	2.2
0.10	10	1.7
0.15	6.67	1.4
0.20	5	1.2

Table 6. Rates of Hydrogenation of Diphenylacetylene to (*Z*)-Stilbene for a Variety of Platinum and Ruthenium Complexes at 50 °C and 1 atm of Hydrogen

compd	reaction time (h)	product (*Z*)-stilbene (turnover no.)	product (*E*)-stilbene (turnover no.)	turnover freq for formation of (*Z*)-stilbene
$Pt(PhC_2Ph)_2$	20.0	21.8	0	1.1
$Ru_3(CO)_{12}$	17.5	39.3	28	2.2
$Ru(CO)_5$	4.5	20.5	11.9	4.6
$H_2Ru_3(CO)_9(PhC_2Ph)$	15	3.5	4.8	0.2
$HRu_3(CO)_9(\mu_3\text{-ampy})$	4	12.3	3.2	3.0
$PtRu_2(CO)_8(PhC_2Ph)$-(dppe)	18.5	60	5.0	3.2
3a	14	43.0	0	3.0
4	1	1.8	0	1.8
5	11	6.7	2.5	0.6
$Pt_5(CO)_6(PPh_3)_4$[a]	20	58	*a*	2.9

[a] At 50 °C and 50 atm of hydrogen, greater than 95% (*Z*)-stilbene. See ref 16.

CO Dependence Measurements. Mixtures of CO and H_2 with CO composition ranging from 5% to 20% were prepared by adding the appropriate amounts of the two gases to an empty Parr high-pressure vessel. PhC_2Ph (46.0 mg, 0.259 mmol) and 5.0 mg of **1a** (0.002 59 mmol) were dissolved in 1.5 mL of CH_2Cl_2 and 24.5 mL of hexane. The hydrogenation experiments were performed under the standard conditions. The reaction flask was first filled with the H_2/CO gas mixture. It was then slowly purged through the flask at 1 atm during the course of the reaction. The rate was determined by the amount of formation of (*Z*)-stilbene by GLC after the first 1 h of reaction. The results are listed in Table 5.

Temperature Dependence Measurements. A 5.0-mg amount of **1a** (0.002 59 mmol) and 46.0 mg of PhC_2Ph (0.259 mmol) were dissolved in 1.5 mL of CH_2Cl_2 and 24.5 mL of hexane. The hydrogenation measurements were carried out at five different temperatures following the standard procedures. k_{obs} values were obtained by measuring the consumption of PhC_2Ph as a function of time. The activation parameters, $\Delta H^* = 24.9(6)$ kcal/mol and $\Delta S^* = 1.4(9)$ eu, were determined from an average of two sets of data. The given errors are defined as the difference between the values determined for the two independent sets of data.

Catalytic Activity of Related Complexes. The catalytic activities of several pertinent platinum and ruthenium compounds toward hydrogenation of PhC_2Ph were tested under conditions identical to those of **1a**,**b**. These results are listed in Table 6.

Effect of Mercury on Catalytic Activity of 1a. A 46.0-mg amount of PhC_2Ph (0.259 mmol) and a 5.0-mg amount of **1a** (0.00259 mmol) were dissolved in 1.5 mL of CH_2Cl_2 and 24.5 mL of hexane. Mercury (6.0

Table 7. Crystallographic Data for Compounds **2a**, **3b**, and **4**

compd	**2a**	**3b**	**4**
empirical formula	$Pt_3Ru_6O_{18}C_{32}H_{18}$	$Pt_3Ru_6O_{18}C_{34}H_{22}$	$Pt_3Ru_6O_{15}C_{57}H_{36}\cdot C_6H_{14}$
formula weight	1882.17	1910.23	2238.77
crystal system	monoclinic	monoclinic	monoclinic
lattice params			
a (Å)	16.648(3)	17.192(3)	13.567(2)
b (Å)	14.065(3)	12.126(3)	36.282(9)
c (Å)	17.558(3)	22.649(4)	13.711(2)
β (deg)	92.78(1)	111.98(1)	99.09(1)
V (Å^3)	4106(1)	4378(2)	6664(2)
space group	$P2_1/n$ (No. 14)	$P2_1/n$ (No. 14)	$P2_1/n$ (No. 14)
Z	4	4	4
D_{calcd} g/cm^3	3.04	2.90	2.3
μ(Mo Kα) cm^{-1}	124.6	116.9	76.9
temp (°C)	20	20	20
$2\theta_{max}$ (deg)	41.0	40.0	40.0
no. of obs. reflns ($I > 3\sigma(I)$)	2625	3023	4178
no. of variables	372	562	544
residuals (R; R_w)	0.033; 0.032	0.028; 0.029	0.049; 0.046
goodness of fit indicator	1.12	1.33	2.30
max shift in final cycle	0.15	0.04	0.12
largest peak in final diff map, e$^-$ (Å^3)	0.99	0.57	1.18
abs corr	empirical	DIFABS	DIFABS
trans coeff (max/min)	1.00/0.62	1.00/0.63	1.67/0.75

g) was then added to the flask, and the hydrogenation was then carried out under the usual conditions. The reaction was followed by GLC for a period of 2 h. The turnover number for formation of (*Z*)-stilbene was 47(1) at the end of the first 1 h, indicating that there was no measurable inhibition of the catalysis by the mercury. The solution was separated from the mercury, and 3.1 mg of **1a** was recovered by TLC. No other complexes were observed.

Labeling Experiments. Hydrogenation of TolC$_2$Tol by 1a. A 32.0-mg amount of TolC$_2$Tol (0.155 mmol) and 10.0 mg of **1a** (0.005 18) mmol) were dissolved in 3.0 mL of CH_2Cl_2 and 49.0 mL of hexane. The hydrogenation was then performed under the usual conditions, and the reaction was stopped at 20.0 min. A GLC analysis of the reaction solution showed that 14.6% (4.5 turnovers) of the TolC$_2$Tol was reduced to (*Z*)-Tol(H)C=C(H)Tol. Separation of the metal complexes by TLC (hexane/CH_2Cl_2 (3/1)) yielded 5.1 mg of **1b** and 3.2 mg of **1a**. A small amount of (*Z*)-stilbene was also observed.

Reaction of 1a with TolC$_2$Tol in the Absence of Hydrogen. A 5.0-mg amount of **1a** (0.002 59 mmol) and a 16.0-mg amount of TolC$_2$Tol (0.0776 mmol) were dissolved in 1.5 mL of CH_2Cl_2 and 24.5 mL of hexane in a three-necked 25-mL flask with a stir bar. The flask was then placed in an oil bath at 50 °C for 20.0 min. After cooling, the solvent was removed and the residue was separated by TLC (hexane/CH_2Cl_2 (3/1)), affording 4.5 mg of unreacted **1a** (90%). There was no evidence for the formation of **1b**.

Deuteration of TolC$_2$Tol using 1b as the Catalyst. A 16.0-mg amount of TolC$_2$Tol (0.0776 mmol) and **1b** (5.0 mg, 0.002 55 mmol) were dissolved in 1.5 mL of CH_2Cl_2 and 24.5 mL of hexane. The reaction with deuterium was performed under the usual hydrogenation conditions except a temperature of 40 °C was used. The reaction was stopped after 1 h. GLC analysis showed that 14.3% (4.3 turnovers) of the TolC$_2$Tol was converted to (*Z*)-TolC$_2$D$_2$Tol. A total of 4.4 mg of **1b** (88%) was recovered after separation by TLC. A ^{1}H NMR spectrum of the recovered **1b** showed that compared to the methyl resonances the hydride resonances possessed only 36% of the intensity they had before this reaction.

Reaction of 1b with D$_2$. A 10.0-mg amount of **1b** (0.005 10 mmol) was dissolved in 3.0 mL of CH_2Cl_2 and 49.0 mL of hexane in a three-necked 50-mL flask with a stir bar. The solution was purged with D_2 at 40 °C for 1 h. After the solvent was removed, an ^{1}H NMR spectrum of the **1b** at −90 °C showed the intensities of hydride resonances were 91% of their original value.

A Test for Isotope Effect. A 10.0-mg amount of **1a** and 92.0 mg of PhC$_2$Ph were dissolved in 3.0 mL of CH_2Cl_2 and 49.0 mL of hexane, and deuteration using D_2 was performed under standard conditions. After 1 h of reaction time, 47% of PhC$_2$Ph was converted to (*Z*)-PhC(D)=C(D)Ph. The rate for the formation of (*Z*)-PhC(D)=C(D)Ph is thus indistinguishable from that of the formation of (*Z*)-PhC(H)=C(H)Ph from H_2 by this catalyst.

Isomerization of 2a to 3a. A 1.5-mg amount of **2a** was dissolved in 0.8 mL of toluene-d_8 in an NMR tube, and the ^{1}H NMR spectrum was recorded. The NMR tube was evacuated and filled with nitrogen and then immersed in an oil bath at 65 °C for 5.5 h. An ^{1}H NMR spectrum was recorded again and showed the formation of **3a**. Separation by TLC yielded 0.8 mg of **3a** and a trace amount (0.1 mg) of **2a**.

Transformation of 4 to Ru$_6$Pt$_3$(CO)$_{14}$(μ_3-PhC$_2$Ph)$_3$ (5). A 5.0-mg amount of **4** (0.002 32 mmol) was dissolved in 20.0 mL of hexane in a three-necked 50-mL flask with a stir bar. The solution was heated to reflux for 1 h. After cooling, the solvent was removed and the residue was separated by TLC (hexane/CH_2Cl_2 (2/1)), to yield 1.5 mg of unreacted **4** (30%) and 1.8 mg of **5** (37%).

Crystallographic Analyses. Crystals of compound **2a** suitable for X-ray diffraction analysis were obtained by slow evaporation of solvent from solutions in hexane/CH_2Cl_2 (1/5) solvent mixtures at 25 °C. Crystals of compound **3b** were obtained by slow evaporation of solvent from solutions in benzene/octane (4/1) solvent mixtures at 25 °C. Crystals of compound **4** were obtained by slow evaporation of solvent from solutions in hexane/CH_2Cl_2 (1/2) solvent mixtures at 25 °C. All crystals used in the data collections were mounted in thin-walled glass capillaries. Diffraction measurements were made on a Rigaku AFC6S automatic diffractometer by using graphite-monochromated Mo Kα radiation. The unit cells were determined and refined from 25 randomly selected reflections obtained by using the automatic search, center, index, and least-squares routines. Crystal data, data collection parameters, and results of the analyses are listed in Table 7. All data processing was performed on a Digital Equipment Corp. VAXstation 3520 computer by using the TEXSAN structure solving program library (version 2.0) obtained from Molecular Structure Corp., The Woodlands, TX. Neutral-atom scattering factors were obtained from the standard source.[13a] Anomalous dispersion corrections were applied to all non-hydrogen atoms.[13b] For all analyses, the positions of the metal atoms were determined by direct methods (MITHRIL), and all other non-hydrogen atomic positions were obtained from subsequent difference Fourier syntheses.

All three compounds crystallized in the monoclinic crystal system in the space group $P2_1/n$. The space group was established uniquely from the patterns of systematic absences observed in the data in each case. The structure was solved by a combination of direct methods (MITHRIL) and difference Fourier techniques.

For **2a**, all atoms heavier than carbon were refined with anisotropic thermal parameters. The positions of the hydride ligands were calculated by using the energy minimization program HYDEX, M–H = 1.90 Å.[13] The positions of the hydrogen atoms on the hydrocarbon ligands were calculated, C – H = 0.95 Å. For **3b**, all non-hydrogen atoms were refined with anisotropic thermal parameters. All four hydride ligands were located and refined. The positions of the hydrogen atoms on the diphenylethane ligand were calculated assuming idealized geometries. All hydrogen atom positions on the ligands were included in the structure factor calculations, but they were not refined.

(13) (a) *International Tables for X-ray Crystallography*; Kynoch Press: Birmingham, England, 1975; Vol. IV, Table 2.2B, pp 99–101. (b) *Ibid.* Table 2.3.1, pp 149–150.

For **4**, all non-hydrogen atoms were refined with anisotropic thermal parameters except for the carbon atoms of the alkyne ligands, which were refined with isotropic thermal parameters. A molecule of hexane that had cocrystallized from the crystallization solvent was found in the crystal in the final stages of the analysis. It was included in the analysis and satisfactorily refined with isotropic thermal parameters for the carbon atoms. Four of the six hydride ligands were located and partially refined in sites bridging metal–metal bonds. Two hydride ligands, H(3) and H(4), could not be located. The positions for these two ligands were subsequently calculated in bridging sites analogous to those of the other four by using the energy minimization program HYDEX, M–H = 1.80 Å.[14] The positions of the hydrogen atoms on the hydrocarbon ligands were calculated, C–H = 0.95 Å. On the final cycles of refinement, all hydrogen atom positions were included in the structure factor calculations without refinement.

Results

Diphenylacetylene is hydrogenated to (*Z*)-stilbene by **1a** with high selectivity in solvent mixtures of methylene chloride and hexane at 50 °C under hydrogen at 1 atm. At a PhC_2Ph (10^{-2} M) to **1a** (10^{-4} M) ratio of 100/1, 47 equiv of (*Z*)-stilbene were formed after 1 h, corresponding to a turnover frequency (TOF, mol of product/(mol of catalyst·h)) of 47. After 3 h, 81% of the PhC_2Ph was converted to (*Z*)-stilbene and 4% to (*E*)-stilbene. A trace of 1,2-diphenylethane was observed, and 15% of the PhC_2Ph was recovered. Separation of the metal-containing complexes yielded **1a** (49%), a trace amount of the known compound $Ru_6Pt_3(CO)_{14}(\mu_3\text{-}PhC_2Ph)_3$[11] (**5**), and two new compounds $Ru_6Pt_3(CO)_{18}(\mu_3\text{-}\eta^6\text{-}PhC_2H_4Ph)(\mu\text{-}H)_4$ (**2a**) and $Ru_6Pt_3(CO)_{18}(\eta^6\text{-}PhCH_2CH_2Ph)(\mu\text{-}H)_4$ (**3a**) as a mixture of isomers (combined yield of 18%). The latter isomers can be separated by repeated application of TLC techniques, but some material is lost. Compound **2a** slowly isomerizes to **3a** over a period of time. The conversion is approximately 50% after 5.5 h at 65 °C. The catalytic activity of compound **3a** for hydrogenation of diphenylacetylene to (*Z*)-stilbene was measured independently, and a TOF of approximately 3.0 h^{-1} was determined under the conditions used for **1a**.

To assess the long-term stability of the catalyst, a reaction was also studied using a 1000/1 PhC_2Ph/**1a** ratio at 50 °C and a 10^{-4} M concentration of **1a**. The reaction was followed for a period of 13 h. At the end of the 13-h period, the metal complexes were then separated by TLC to yield **1a** (9% recovered), the new compound $Ru_6Pt_3(CO)_{15}(\mu_3\text{-}PhC_2Ph)_3(\mu\text{-}H)_6$ (**4**) (22% yield), $Ru_6Pt_3(CO)_{14}(\mu_3\text{-}PhC_2Ph)_3$[11] (**5**) (15% yield), and a mixture of **2a** and **3a** (11% combined yield). Compound **4** was fully characterized by IR, ^1H NMR, and a single crystal X-ray diffraction analysis. In an independent reaction, it was shown that compound **4** can be converted to **5** in 37% yield by heating a solution in hexane solvent to reflux for 1 h.

A plot of the formation of (*Z*)-stilbene in turnovers as a function of time for this reaction is shown in Figure 1. A total of 493 turnovers (TN) was obtained. As one can see, the formation of (*Z*)-stilbene nearly ceases in the final hours of the experiment. Also, it is also notable that there is little or no induction period before the formation of the (*Z*)-stilbene begins.

A plot of the reaction rate in TOF for the formation of (*Z*)-stilbene as a function of time for this reaction is shown in Figure 2. This plot shows that the rate is quite significant in the first 2 h (TOF ≈ 80 h^{-1}) but steadily declines and is no more than 6 h^{-1} at the end of the 13-h period. This can be attributed to the progressive degradation of the catalyst, and only 9% of the **1a** could be recovered at the end of the 13-h period.

The low solubility of **1a** in hexane solvent was a problem. To increase the solubility, methylene chloride was added to the reaction solutions. Methylene chloride/hexane ratios less than 3/49 resulted in lower TOFs for (*Z*)-stilbene formation because not all of the **1a** was dissolved. At higher methylene chloride/hexane ratios, TOFs similar to the 3/49 ratio were obtained.

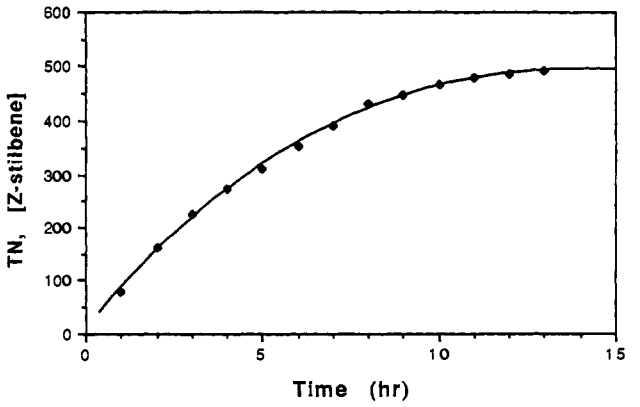

Figure 1. Plot of the formation of (*Z*)-stilbene represented by turnover numbers (TN) as a function of time.

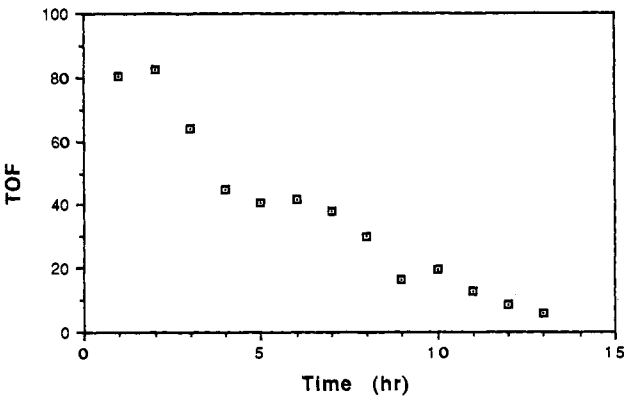

Figure 2. Plot of the rate of formation of (*Z*)-stilbene represented by turnover freqency (TOF) as a function of time.

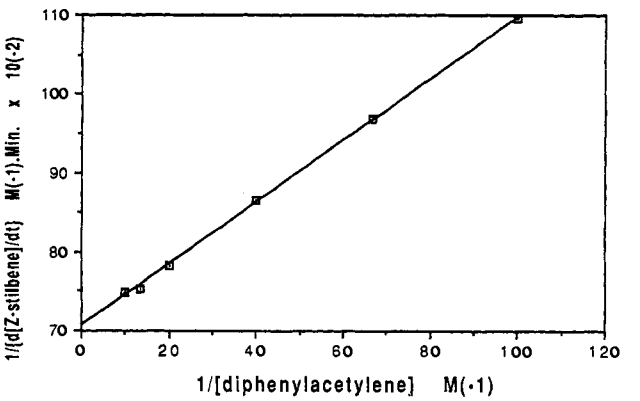

Figure 3. Plot of 1/rate of the formation of (*Z*)-stilbene as a function of $1/[PhC_2Ph]$.

The TOF for the catalytic hydrogenation of $TolC_2Tol$ to (*Z*)-Tol(H)C=C(H)Tol by **1b** was determined to be 30(1) h^{-1}. The compound $Ru_6Pt_3(CO)_{18}(\eta^6\text{-}TolCH_2CH_2Tol)(\mu_3\text{-}H)_4$ (**3b**) was obtained from these reactions in about 10% yield after 2 h. No **2b** was detected. The structures of both **2a** and **3b** were determined by single crystal X-ray diffraction analyses. These results will be described below.

Kinetic Studies. The dependence of the rate on the alkyne concentration was investigated over the range 10^{-1}–10^{-2} M with the concentration of **1a** at 10^{-4} M. An inverse plot (1/rate vs $1/[PhC_2Ph]$) of these results is shown in Figure 3. The results obey the relationship $1/R = A(1/[\text{alkyne}]) + B$ and contain a substantial intercept *B*. The corresponding direct relationship is

(14) Orpen, A. G. *J. Chem. Soc., Dalton Trans.* **1980**, 2509.
(15) Anton, D. R.; Crabtree, R. H. *Organometallics* **1983**, *2*, 855.
(16) Fusi, A.; Ugo, R.; Psaro, R.; Braunstein, P.; Dehand, J. *J. Mol. Catal.* **1982**, *16*, 217.

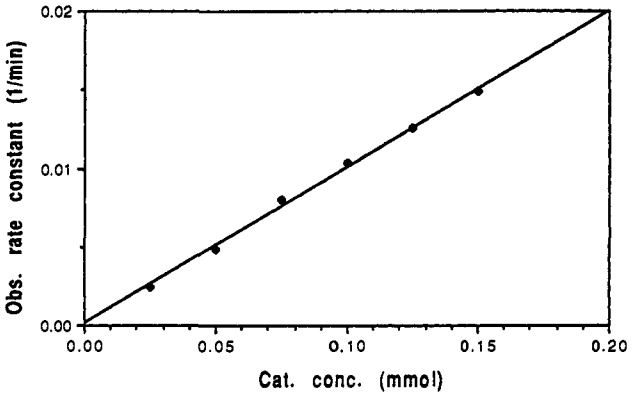

Figure 4. Plot of the rate of disappearance of PhC_2Ph as a function of the concentration of **1a**.

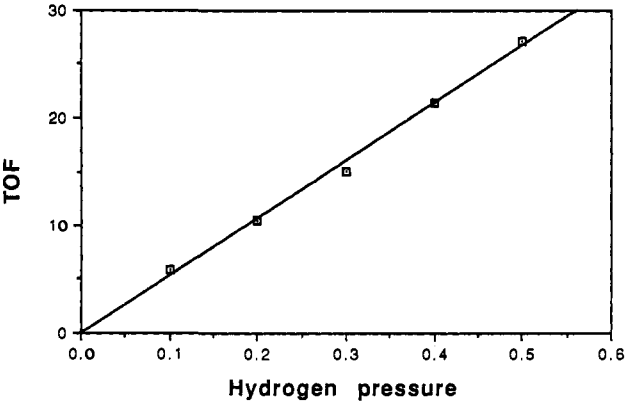

Figure 5. Plot of the rate of formation of (*Z*)-stilbene represented by turnover frequency (TOF) as a function of the partial pressure of hydrogen, $p(H_2)$.

R = [alkyne]/(A + B[alkyne])), which shows that there is both a direct and inverse dependence of the rate on the alkyne concentration.

Our measurements show that the rate of hydrogenation of PhC_2Ph exhibits a linear first-order dependence on the concentration of **1a** in the range (0.25–1.5) × 10^{-4} M. A plot of these results is shown in Figure 4.

The rates of hydrogenation as a function of the partial pressure of hydrogen in the range 0.10–0.50 atm were measured with the concentration of **1a** at 10^{-4} M. There is a linear first-order dependence through this range, and a plot of the TOF versus the partial pressure of hydrogen is shown in Figure 5. The inverse plot showed no significant intercept, and therefore there seems to be no significant hydrogen inhibition effect in this pressure range.

It was found that the rate of hydrogenation is strongly inhibited by CO, and a study of the inhibition using a series of hydrogen and CO gas mixtures was conducted from the range 5% CO to 20% CO. A plot of the TOF as function of 1/partial pressure of CO is shown in Figure 6. As can be seen, the CO inhibition in this range is first order in the partial pressure of CO. As a result of the combination of these measurements, the rate equation (eq 1) has been established.

$$\text{rate} = -\mathrm{d}[Ph_2C_2]/\mathrm{d}t = \frac{k_{obs}[1a][\text{alkyne}]p(H_2)}{p(CO)(1 + [\text{alkyne}])} \quad (1)$$

An investigation of the effect of temperature on the rate of catalysis was conducted at five different temperatures. A plot of ln k/T as a functuion of $1/T$ was linear as expected and provided the activation parameters ΔH^* = 24.9(6) kcal/mol and ΔS^* = 1.4(9) eu (Figure 7).

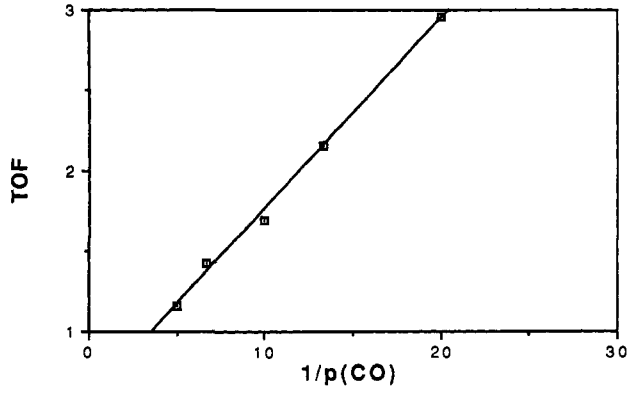

Figure 6. Plot of the rate of formation of (*Z*)-stilbene represented by the turnover frequency (TOF) as a function of the inverse of the partial pressure of carbon monoxide, p(CO).

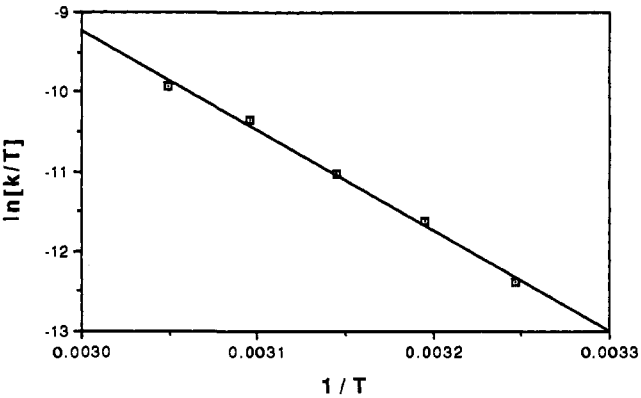

Figure 7. Plot of the rate of formation of (*Z*)-stilbene (ln k/T) as a function of the inverse of the absolute temperature ($1/T$).

Labeling Tests. Two labeling experiments were conducted for the purpose of tracing the flow of the reagents through the catalyst. These were done in the following ways:

(1) The hydrogenation of $TolC_2Tol$ by **1a** was initiated and terminated within 20 min in order to determine the degree of incorporation of the $TolC_2Tol$ into **1a** in the early stages of the reaction. As expected, this results in the transformation of **1a** to **1b**, and the amount of **1b** relative to **1a** was measured at the end of the test period by separating the complexes by TLC and weighing. The results showed the transformation of over 50% of the **1a** to **1b** in this short reaction period. Analysis of the reaction solution showed that 14.6% (4.5 turnovers) of the $TolC_2Tol$ was reduced to (*Z*)-Tol(H)C=C(H)Tol. A small amount of (*Z*)-stilbene was also observed. Most importantly, a control experiment showed that *no* **1b** was formed when **1a** was allowed to react with $TolC_2Tol$ in the absence of hydrogen in the same period of time under similar conditions.

(2) To monitor the flow of hydrogen through the catalyst, the deuteration of $TolC_2Tol$ was performed by using undeuterated **1b** as the catalyst precursor. This reaction was conducted at 40 °C and was stopped after 1 h. Analysis of the solution showed that 14.3% (4.3 turnovers) of the $TolC_2Tol$ was reduced to (*Z*)-Tol(D)C=C(D)Tol. The amount of deuterium incorporation in the recovered **1b** was determined by ^{1}H NMR spectroscopy, which showed that the intensity of hydride signals relative to that of the methyl groups was only 36% of the original value. This is interpreted as 64% deuterium incorporation. In a control experiment, **1b** was allowed to react with D_2 in the absence of $TolC_2Tol$ at 40 °C for 1 h. The recovered **1b** showed the intensity of the hydride resonances was 91% of their original value. This is interpreted to indicate that there is a slow exchange of deuterium with hydrogen in the absence of the alkyne, but the rate is *significantly enhanced* in the presence of alkyne hydrogenation.

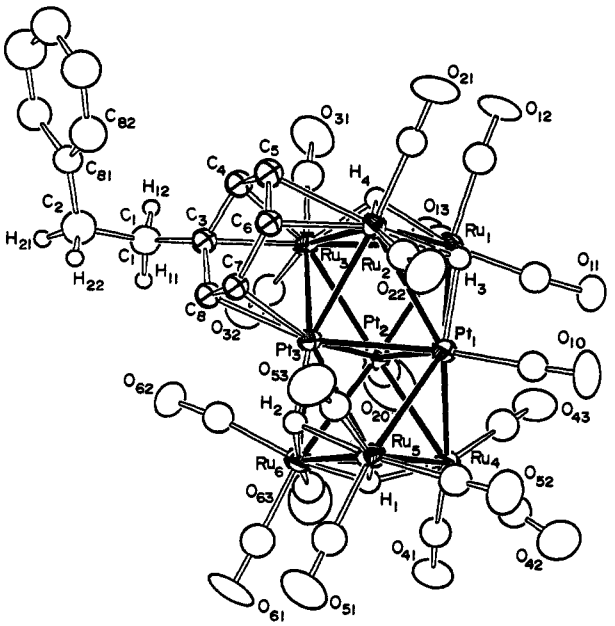

Figure 8. ORTEP diagram of $Ru_6Pt_3(CO)_{18}(\mu_3\text{-}\eta^6\text{-}PhC_2H_4Ph)(\mu_3\text{-}H)_4$ (**2a**) showing 35% probability thermal ellipsoids for the non-hydrogen atoms.

Table 8. Intramolecular Distance for **2a**[a]

atom	atom	distance	atom	atom	distance
Pt(1)	Pt(2)	2.673(1)	Pt(3)	Ru(2)	2.714(2)
Pt(1)	Pt(3)	2.641(1)	Pt(3)	Ru(3)	2.727(2)
Pt(1)	Ru(1)	2.871(2)	Pt(3)	Ru(5)	2.879(2)
Pt(1)	Ru(2)	2.924(2)	Pt(3)	Ru(6)	2.868(2)
Pt(1)	Ru(4)	2.729(2)	Ru(1)	Ru(2)	2.979(2)
Pt(1)	Ru(5)	2.778(2)	Ru(1)	Ru(3)	2.932(3)
Pt(2)	Pt(3)	2.635(1)	Ru(2)	Ru(3)	2.953(3)
Pt(2)	Ru(1)	2.813(2)	Ru(4)	Ru(5)	3.026(2)
Pt(2)	Ru(3)	2.807(2)	Ru(4)	Ru(6)	2.987(3)
Pt(2)	Ru(4)	2.752(2)	Ru(5)	Ru(6)	3.027(3)
Pt(2)	Ru(6)	2.785(2)	C(1)	C(2)	1.54(3)

[a] Distances are in angstroms. Estimated standard deviations in the least significant figure are given in parentheses.

$Ru_6Pt_3(CO)_{18}(\mu_3\text{-}\eta^6\text{-}PhC_2H_4Ph)(\mu_3\text{-}H)_4$ (2a). Compound **2a** was characterized by a single crystal X-ray diffraction analysis, and an ORTEP diagram of its molecular structure is shown in Figure 8. Selected bond distances and angles are given in Tables 8 and 9, respectively. This compound contains a layered structure of Pt_3 and Ru_3 triangles that is similar to that in **1a**. The Pt–Pt distances range from 2.635(1) to 2.673(1) Å and are very similar to those of **1a**, 2.631(1)–2.686(1) Å, and the related compounds $Pt_3Ru_6(CO)_{21}(\mu\text{-}H)_3(\mu_3\text{-}H)$ (**6**), 2.629(1)–2.646(1) Å, and

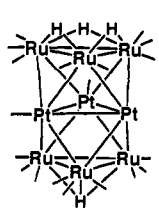

6

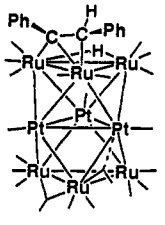

7

$Pt_3Ru_6(CO)_{21}[\mu\text{-}PhCC(H)Ph](\mu\text{-}Ph](\mu\text{-}H)$ (**7**), 2.614(2)–2.742(2) Å.[6] The Pt–Ru distances span a wide range, 2.714(2)–2.924(2) Å. This is due in part to the effects of the bridging hydride ligands which are known to cause lengthening of the associated metal–metal bonds.[17] All Ru–Ru bond distances are long, 2.932(3)–3.027(3) Å, and this too is due to the effect of the bridging hydride ligands, see below. There is a triply bridging diphenylethane ligand that is coordinated in a triply bridging $\eta^2\text{:}\eta^2\text{:}\eta^2$-fashion to one of the $PtRu_2$ triangular groups, Pt(3), Ru(2), and Ru(3), through one of its phenyl groups. Triply bridging arene ligands have been reported previously.[18] There does not appear to be an alternating pattern of long and short C–C distances in the coordinated ring as has been found in other $\mu_3\text{-}\eta^2\text{:}\eta^2\text{:}\eta^2$-arene complexes.[18] The compound **2a** appears to contain four hydride ligands. This conclusion is based largely on the fact that it is thermally converted to its isomer **3a**, which like **3b** has four hydride ligands, see below. Also, according to the electron counting rules, compound **2a** should contain 124 cluster valence electrons as a face-shared bioctahedron and would need four hydride ligands to achieve this electron count.[19] The hydride ligands were not located directly in the crystal structure analysis, and an elemental analysis of pure **2a** was not possible because it is obtained only in very small amounts and is continuously isomerizing to **3a**. The ^1H NMR spectrum indicated the presence of four hydride ligands, but this molecule exists in solution as a mixture of isomers and is dynamically active on the NMR time scale at room temperature; thus, the accuracy of the resonance integrations was not as accurate as usual. Only a single broad resonance, $\delta = -16.18$ ppm ($\Delta\nu_{1/2} = 370$ Hz), was observed for the hydride ligands at room temperature. The general locations for the four hydride ligands shown in Figure 8 were selected using the criterion that bridging hydride ligands cause lengthening of the associated metal–metal bonds. The exact positions were then selected using the energy minimization program HYDEX. By this process, all four hydride ligands were positioned in triply bridging sites. H(1) and H(4) bridge the two Ru_3 triangles. Hydride ligands bridging Ru_3 triangles were also observed in compounds **1a** and **6**. Hydrides H(2) and H(3) were positioned on $PtRu_2$ triangles. These ligands are associated with the four longest Pt–Ru bonds. In addition to the broad hydride resonance at −16.18 ppm, other resonances in the ^1H NMR spectrum include a multiplet at 7.25–7.50 ppm (5H) due to the uncoordinated phenyl group, a triplet at 4.61 ppm (1H) and multiplet at 4.26–4.26 ppm (4H) due to the coordinated phenyl grouping, and two mutually coupled triplets at 3.16 ppm (2H, $^3J_{H\text{-}H} = 7.0$ Hz) and 2.83 (2H, $^3J_{H\text{-}H} = 7.0$ Hz) due to the methylene groups of the diphenylethane ligand.

Table 9. Intramolecular Bond Angles for **2a**[a]

atom	atom	atom	angle	atom	atom	atom	angle
Pt(2)	Pt(1)	Ru(2)	91.21(5)	Ru(2)	Pt(3)	Ru(6)	154.97(6)
Pt(2)	Pt(1)	Ru(5)	94.44(5)	Ru(3)	Pt(3)	Ru(5)	154.00(6)
Pt(3)	Pt(1)	Ru(1)	88.98(5)	Ru(3)	Pt(3)	Ru(6)	108.11(6)
Pt(3)	Pt(1)	Ru(4)	95.39(5)	Pt(1)	Ru(1)	Ru(3)	87.76(6)
Ru(1)	Pt(1)	Ru(4)	108.26(6)	Pt(2)	Ru(1)	Ru(2)	87.39(6)
Ru(1)	Pt(1)	Ru(5)	151.08(6)	Pt(1)	Ru(2)	Ru(3)	86.37(6)
Ru(2)	Pt(1)	Ru(4)	150.12(6)	Pt(3)	Ru(2)	Ru(1)	85.41(6)
Ru(2)	Pt(1)	Ru(5)	107.45(5)	Pt(2)	Ru(3)	Ru(2)	88.01(6)
Pt(1)	Pt(2)	Ru(3)	94.42(5)	Pt(3)	Ru(3)	Ru(1)	86.12(6)
Pt(1)	Pt(2)	Ru(6)	92.85(5)	Pt(1)	Ru(4)	Ru(6)	87.43(6)
Pt(3)	Pt(2)	Ru(1)	90.33(5)	Pt(2)	Ru(4)	Ru(5)	87.52(6)
Pt(3)	Pt(2)	Ru(4)	94.97(5)	Pt(1)	Ru(5)	Ru(6)	85.77(6)
Ru(1)	Pt(2)	Ru(4)	109.27(6)	Pt(3)	Ru(5)	Ru(4)	84.51(6)
Ru(1)	Pt(2)	Ru(6)	151.96(6)	Pt(2)	Ru(6)	Ru(5)	86.93(6)
Ru(3)	Pt(2)	Ru(4)	152.32(6)	Pt(3)	Ru(6)	Ru(4)	85.41(6)
Ru(3)	Pt(2)	Ru(6)	108.23(6)	C(2)	C(1)	C(3)	112(2)
Pt(1)	Pt(3)	Ru(3)	97.05(5)	C(1)	C(2)	C(81)	115(2)
Pt(1)	Pt(3)	Ru(6)	91.65(5)	Pt	C	O(av)	176(2)
Pt(2)	Pt(3)	Ru(2)	96.87(5)	Ru	C	O(av)	175(2)
Pt(2)	Pt(3)	Ru(5)	92.94(5)				
Ru(2)	Pt(3)	Ru(5)	110.56(6)				

[a] Angles are in degrees. Estimated standard deviations in the least significant figure are given in parentheses.

(17) Bau, R. *Struct. Bonding* **1981**, *44*, 1.

(18) Dyson, P. J.; Johnson, B. F. G.; Lewis, J.; Matinelli, M.; Braga, D.; Grepioni, F. *J. Am. Chem. Soc.* **1993**, *115*, 9062.

(19) Mingos, D. M. P.; May, A. S. In *The Chemistry of Metal Cluster Complexes*; Shriver, D. F., Kaesz, H. D., Adams, R. D., Eds.; VCH Publishers: New York, 1990; Chapter 2.

The variable-temperature ^1H NMR spectra showed a complex series of changes at lower temperatures than can best be explained as involving a combination of two dynamical processes. (1) The simplest process involves the broadening and separation of the two triplets of the two methylene groups into two pairs of broad resonances of similar intensities that are observed at approximately 3.17 and 2.92 ppm and 3.10 and 2.45 ppm (no couplings were seen on these broad resonances). Mechanistically, this is attributed to the slowing of a process that averages two conformational isomers formed by rotation of the μ_3-η^2:η^2:η^2-phenyl on an axis perpendicular to the C_6 plane. One of these isomers is believed to be the one shown Figure 8. The other would be one of two possibilities: one where the CH_2CH_2Ph-substituted carbon occupies the site shown as C(4) in Figure 8 or where the CH_2CH_2Ph-substituted carbon occupies the site shown as C(8) in Figure 8. We feel that the latter is less likely because of steric interactions with the carbonyl group, C(62)–O(62). Isomers with the CH_2CH_2Ph group at other phenyl carbon sites shown in Figure 8 would be equivalent to these three in the presence of rapid scrambling of the hydride ligands, and that is the other dynamical process, see below. As expected, this process also produces changes in the resonances of the coordinated and uncoordinated phenyl groups as a function of temperature, but these changes are complex and uninterpretable. (2) For two isomers, one should see a maximum of eight hydride resonances, if hydride scrambling is not occurring. At the lowest temperature that we could record (−90 °C in CD_2Cl_2 solvent), we observed only five: two pairs of broad resonances at 13.65 and 14.10 ppm and 15.50 and 19.80 ppm. The former pair has approximately one-half the intensity of the latter. In addition, there is a sharp singlet at 16.20 ppm. As the temperature is raised, all of the resonances broaden and coalesce into the single broad resonance at −16.18 ppm observed at room temperature. Since only five resonances were observed at −90 °C, it is believed that some rapid averaging is still occurring on the NMR time scale even at this temperature. As a result, unambiguous resonance assignments and line shape analyses could not be performed. It is clear however that rapid hydride scrambling is occurring. Rapid scrambling of the hydride ligands was also observed for compounds **1a**,[6] **3b** (see below), and **6**.[11]

$Ru_6Pt_3(CO)_{18}(\eta^6$-PhCH$_2$CH$_2$Ph$)(\mu_3$-H$)_4$ (3a) and $Ru_6Pt_3(CO)_{18}(\eta^6$-TolCH$_2$CH$_2$Tol$)(\mu_3$-H$)_4$ (3b). Compound **3b** provided us with good quality single crystals and was thus characterized by a single crystal X-ray diffraction analysis. An ORTEP diagram of its molecular structure is shown in Figure 9. Selected bond distances and angles are given in Tables 10 and 11, respectively. This compound also contains a layered structure of Pt_3 and Ru_3 triangles that is similar to that found in compounds **1a**, **2a**, **6**, and **7**. The Pt–Pt distances are similar to those found in compounds **1a**, **2a**, **6**, and **7**, ranging from 2.647(1) to 2.675(1) Å. The Pt–Ru distances span a wide range, 2.709(2)–2.974(2) Å. This compound contains four hydride ligands. All were located and refined in the structural analysis. They all occupy triply bridging positions in the cluster. **H(1)** and **H(4)** are triply bridging ligands on each of the Ru_3 triangles. H(2) and **H(3)** are triple bridges on the two adjacent $PtRu_2$ triangles, Pt(1)–Ru(1)–Ru(2) and Pt(3)–Ru(2)–Ru(3), respectively. Note that H(2) and H(3) were *found* to bridge the longest Pt–Ru bonds. The Ru–Ru bonds associated with H(1) and H(4) are also very long but are similar to those found for compounds **1a**, **2a**, and **6**. The molecule contains a 1,2-ditolylethane ligand that is η^6-coordinated to one metal atom only, Ru(2). The complex contains 124 valence electrons and obeys the conventional electron counting rules.[19] The ^1H NMR spectrum at room temperature shows a single resonance of intensity 4 at −14.70 ppm that is flanked by satellites due to coupling to the platinum atoms, J_{Pt-H} = 100 Hz. At −88 °C, this resonance has split into two resonances at −13.52 (3H) and −18.18 (1H) ppm having a 3/1 intensity ratio. Evidently, all of the hydrides are rapidly scrambled at room temperature. At −88 °C, some averaging has been slowed, but three of the hydrides are still being rapidly averaged even at −88 °C. We suspect that the process that has been slowed at −88 °C is the one averaging the remote hydride H(1) with the other three. The methylene resonances were observed as two triplets at 2.92 and 2.62 ppm, $^3J_{H-H}$ = 7.1 Hz.

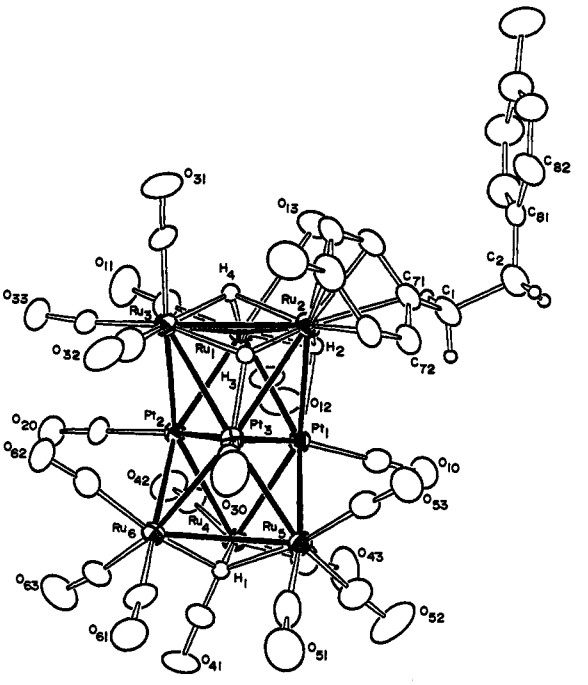

Figure 9. ORTEP diagram of $Ru_6Pt_3(CO)_{18}(\eta^6$-TolCH$_2$CH$_2$Tol$)(\mu_3$-H$)_4$ (**3b**) showing 35% probability thermal ellipsoids for the non-hydrogen atoms.

Table 10. Intramolecular Distances for **3b**[a]

atom	atom	distance	atom	atom	distance
Pt(1)	Pt(2)	2.647(1)	Ru(1)	Ru(2)	2.961(2)
Pt(1)	Pt(3)	2.652(1)	Ru(1)	Ru(3)	2.995(2)
Pt(1)	Ru(1)	2.884(2)	Ru(1)	H(2)	1.8(1)
Pt(1)	Ru(2)	2.910(2)	Ru(1)	H(4)	1.8(1)
Pt(1)	Ru(4)	2.761(2)	Ru(2)	Ru(3)	2.943(2)
Pt(1)	Ru(5)	2.718(2)	Ru(2)	H(2)	1.9(1)
Pt(2)	Pt(3)	2.675(1)	Ru(2)	H(3)	1.7(1)
Pt(2)	Ru(1)	2.785(2)	Ru(3)	H(3)	2.0(1)
Pt(2)	Ru(3)	2.811(2)	Ru(3)	H(4)	1.9(1)
Pt(2)	Ru(4)	2.809(2)	Ru(4)	Ru(5)	2.947(2)
Pt(2)	Ru(6)	2.709(2)	Ru(4)	Ru(6)	2.978(2)
Pt(3)	Ru(2)	2.974(2)	Ru(4)	H(1)	1.9(1)
Pt(3)	Ru(3)	2.904(2)	Ru(5)	Ru(6)	3.067(2)
Pt(3)	Ru(5)	2.716(2)	Ru(5)	H(1)	1.9(1)
Pt(3)	Ru(6)	2.720(2)	Ru(6)	H(1)	1.7(1)
Pt(3)	H(3)	1.8(1)	C(1)	C(2)	1.57(2)

[a] Distances are in angstroms. Estimated standard deviations in the least significant figure are given in parentheses.

Compound **3a** is believed to be structurally analogous to **3b**. Interestingly, the single hydride resonance, δ = −15.34 ppm, observed for this compound in the ^1H NMR spectrum at room temperature shows two pairs of platinum satellites in a two to one ratio, J_{Pt-H} = 77 Hz and J_{Pt-H} = 26 Hz. This is as expected since, even in the presence of rapid hydride scrambling, the platinum atoms remain distinct in two sets in a 2 to 1 ratio. The absence of two sets of satellites in **3b** must mean that the two coupling constants are accidently the same.

$Ru_6Pt_3(CO)_{15}(\mu_3$-PhC$_2$Ph$)_3(\mu$-H$)_6$ (4). Compound **4** was also characterized by a single crystal X-ray diffraction analysis, and an ORTEP diagram of its molecular structure is shown in Figure 10. Selected bond distances and angles are given in Tables 12 and 13, respectively. This compound does not contain a layered

Table 11. Intramolecular Bond Angles for **3b**[a]

atom	atom	atom	angle	atom	atom	atom	angle
Pt(2)	Pt(1)	Ru(2)	91.34(4)	Ru(2)	Pt(3)	Ru(5)	109.83(5)
Pt(2)	Pt(1)	Ru(5)	94.79(4)	Ru(2)	Pt(3)	Ru(6)	148.82(5)
Pt(3)	Pt(1)	Ru(1)	94.50(4)	Ru(3)	Pt(3)	Ru(5)	150.95(5)
Pt(3)	Pt(1)	Ru(4)	92.97(4)	Ru(3)	Pt(3)	Ru(6)	105.20(5)
Ru(1)	Pt(1)	Ru(4)	107.73(5)	Pt(1)	Ru(1)	Ru(3)	86.01(5)
Ru(1)	Pt(1)	Ru(5)	152.44(5)	Pt(2)	Ru(1)	Ru(2)	87.64(5)
Ru(2)	Pt(1)	Ru(4)	152.34(5)	Pt(1)	Ru(2)	Ru(3)	86.48(5)
Ru(2)	Pt(1)	Ru(5)	111.67(5)	Pt(3)	Ru(2)	Ru(1)	86.55(4)
Pt(1)	Pt(2)	Ru(3)	94.51(4)	Pt(2)	Ru(3)	Ru(2)	87.49(5)
Pt(1)	Pt(2)	Ru(6)	94.08(4)	Pt(3)	Ru(3)	Ru(1)	87.19(5)
Pt(3)	Pt(2)	Ru(1)	96.31(4)	Pt(1)	Ru(4)	Ru(6)	86.08(5)
Pt(3)	Pt(2)	Ru(4)	91.41(4)	Pt(2)	Ru(4)	Ru(5)	86.62(5)
Ru(1)	Pt(2)	Ru(4)	109.21(5)	Pt(1)	Ru(5)	Ru(6)	85.09(5)
Ru(1)	Pt(2)	Ru(6)	155.11(5)	Pt(3)	Ru(5)	Ru(4)	87.70(5)
Ru(3)	Pt(2)	Ru(4)	152.42(5)	Pt(2)	Ru(6)	Ru(5)	86.03(5)
Ru(3)	Pt(2)	Ru(6)	108.11(5)	Pt(3)	Ru(6)	Ru(4)	86.99(5)
Pt(1)	Pt(3)	Ru(3)	92.28(4)	C(2)	C(1)	C(71)	111(2)
Pt(1)	Pt(3)	Ru(6)	93.72(4)	C(1)	C(2)	C(81)	116(2)
Pt(2)	Pt(3)	Ru(2)	89.41(4)	Pt	C	O(av)	177(2)
Pt(2)	Pt(3)	Ru(5)	94.21(4)	Ru	C	O(av)	176(2)

[a] Angles are in degrees. Estimated standard deviations in the least significant figure are given in parentheses.

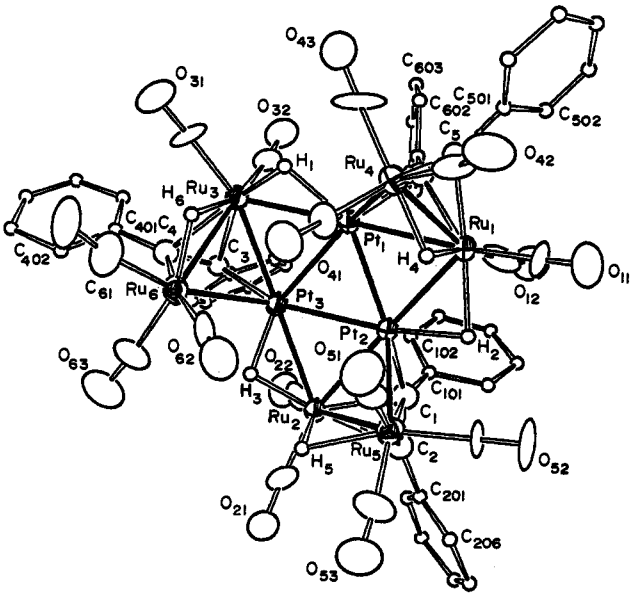

Figure 10. ORTEP diagram of $Ru_6Pt_3(CO)_{15}(\mu_3\text{-}PhC_2Ph)_3(\mu\text{-}H)_6$ (**4**) showing 35% probability thermal ellipsoids for the non-hydrogen atoms.

structure of Pt_3 and Ru_3 triangles. Six of the metal atoms, three ruthenium and three platinum atoms, are arranged in a planar raftlike structure in the form of a triangle of triangles.[20-22] The central triangular group contains the three platinum atoms. Similar structures were found for the complexes $[Pt_3Fe_3(CO)_{15}]^{0,1-,2-}$.[20] The Pt–Pt distances range from 2.695(2)–2.728(1) Å. These distances lie between the lengths found in the monoanion and dianions $[Pt_3Fe_3(CO)_{15}]^{1-}$ and $[Pt_3Fe_3(CO)_{15}]^{2-}$ which contain one and two electrons in the low lying antibonding orbital centered on the Pt_3 triangle.[20b] The three remaining ruthenium atoms are symmetrically disposed about the Pt_3Ru_3 raft and bridge Ru–Pt edges. All three lie out of the plane on the same side and produce an approximate overall C_3 symmetry. Each of the three Ru_2Pt triangles contains a triply bridging PhC_2Ph ligand and one bridging hydride ligand across the Ru–Ru edge. The remaining three hydride ligands bridge Pt–Ru edges in the Pt_3Ru_3 raft. Two hydride resonances at $\delta = -8.59$ and -16.01 ppm of equal intensities corresponding to the two sets of three ligands were observed in a ^1H NMR spectrum recorded at −73 °C. The hydride resonances were not observed at 25 °C, presumably due to dynamical averaging that is occurring at an intermediate rate on the NMR time scale at 25 °C. Probably the most similar compound to compound **4** is $Ru_6Pt_3(CO)_{18}(\mu_3\text{-}PhC_2Ph)_3$ (**8**), which has three more CO ligands and no hydride ligands.[11] Compound **8** contains a central Pt_3 triangle with Ru_2 groups bridging each edge and a triply bridging PhC_2Ph ligand $PtRu_2$ triangles. Compound **4** contains 15 linear terminal carbonyl ligands: the ruthenium atoms in the Pt_3Ru_6 raft have two each

Table 12. Intramolecular Distances for **4**[a]

atom	atom	distance	atom	atom	distance
Pt(1)	Pt(2)	2.702(2)	Ru(1)	C(6)	2.18(2)
Pt(1)	Pt(3)	2.728(1)	Ru(2)	Ru(5)	2.796(3)
Pt(1)	Ru(1)	2.719(2)	Ru(2)	C(1)	2.17(2)
Pt(1)	Ru(3)	2.724(2)	Ru(2)	C(2)	2.17(2)
Pt(1)	Ru(4)	2.705(2)	Ru(3)	Ru(6)	2.795(3)
Pt(1)	C(6)	2.01(2)	Ru(3)	C(3)	2.21(2)
Pt(2)	Pt(3)	2.695(2)	Ru(3)	C(4)	2.24(2)
Pt(2)	Ru(1)	2.727(2)	Ru(4)	C(5)	2.09(2)
Pt(2)	Ru(2)	2.716(2)	Ru(4)	C(6)	2.69(2)
Pt(2)	Ru(5)	2.672(3)	Ru(5)	C(1)	2.60(3)
Pt(2)	C(1)	2.03(2)	Ru(5)	C(2)	2.10(2)
Pt(3)	Ru(2)	2.729(2)	Ru(6)	C(4)	2.07(2)
Pt(3)	Ru(3)	2.711(3)	O	C(av)	1.12(3)
Pt(3)	Ru(6)	2.682(2)	C(1)	C(2)	1.27(3)
Pt(3)	C(3)	2.05(2)	C(3)	C(4)	1.42(3)
Ru(1)	Ru(4)	2.799(3)	C(5)	C(6)	1.41(3)
Ru(1)	C(5)	2.19(2)	C(Ph)	C(av)	1.38(4)

[a] Distances are in angstroms. Estimated standard deviations in the least significant figure are given in parentheses.

Table 13. Intramolecular Bond Angles for **4**[a]

atom	atom	atom	angle	atom	atom	atom	angle
Pt(2)	Pt(1)	Pt(3)	59.50(4)	Pt(1)	Pt(3)	Ru(3)	60.10(5)
Pt(2)	Pt(1)	Ru(1)	60.40(5)	Pt(1)	Pt(3)	Ru(6)	103.17(6)
Pt(2)	Pt(1)	Ru(3)	119.15(6)	Pt(2)	Pt(3)	Ru(2)	60.09(5)
Pt(2)	Pt(1)	Ru(4)	106.77(7)	Pt(2)	Pt(3)	Ru(3)	119.87(6)
Pt(3)	Pt(1)	Ru(1)	119.82(6)	Pt(2)	Pt(3)	Ru(6)	133.83(6)
Pt(3)	Pt(1)	Ru(3)	59.64(5)	Ru(2)	Pt(3)	Ru(3)	177.51(8)
Pt(3)	Pt(1)	Ru(4)	135.86(7)	Ru(2)	Pt(3)	Ru(6)	115.62(8)
Ru(1)	Pt(1)	Ru(3)	177.35(8)	Ru(3)	Pt(3)	Ru(6)	62.42(7)
Ru(1)	Pt(1)	Ru(4)	62.13(7)	Pt(1)	Ru(1)	Pt(2)	59.50(5)
Ru(3)	Pt(1)	Ru(4)	116.21(7)	Pt(1)	Ru(1)	Ru(4)	58.69(7)
Pt(1)	Pt(2)	Pt(3)	60.72(4)	Pt(2)	Ru(1)	Ru(4)	103.52(9)
Pt(1)	Pt(2)	Ru(1)	60.10(6)	Pt(2)	Ru(2)	Pt(3)	59.33(5)
Pt(1)	Pt(2)	Ru(2)	121.22(6)	Pt(2)	Ru(2)	Ru(5)	57.96(6)
Pt(1)	Pt(2)	Ru(5)	136.04(6)	Pt(3)	Ru(2)	Ru(5)	102.86(8)
Pt(3)	Pt(2)	Ru(1)	120.74(7)	Pt(1)	Ru(3)	Pt(3)	60.26(6)
Pt(3)	Pt(2)	Ru(2)	60.58(6)	Pt(1)	Ru(3)	Ru(6)	100.4(1)
Pt(3)	Pt(2)	Ru(5)	107.22(6)	Pt(3)	Ru(3)	Ru(6)	58.27(7)
Ru(1)	Pt(2)	Ru(2)	174.22(8)	Pt(1)	Ru(4)	Ru(1)	59.18(6)
Ru(1)	Pt(2)	Ru(5)	112.33(7)	Pt(2)	Ru(5)	Ru(2)	59.51(7)
Ru(2)	Pt(2)	Ru(5)	62.53(7)	Pt(3)	Ru(6)	Ru(3)	59.31(7)
Pt(1)	Pt(3)	Pt(2)	59.78(4)	Ru	C	O(av)	175(3)
Pt(1)	Pt(3)	Ru(2)	119.79(6)				

[a] Angles are in degrees. Estimated standard deviations in the least significant figure are given in parentheses.

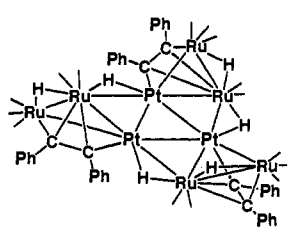

4

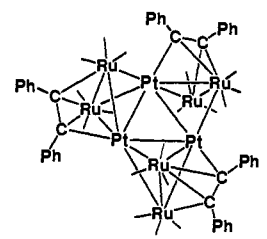

8

(20) (a) Adams, R. D.; Arafa, I.; Chen, G.; Lii, J.-C.; Wang, J.-G. *Organometallics* **1990**, *9*, 2350. (b) Longoni, G.; Manassero, M.; Sansoni, M. *J. Am. Chem. Soc.* **1980**, *102*, 7973.

(21) Goudsmit, R. J.; Johnson, B. F. G.; Lewis, J.; Raithby, P.; Whitmire, K. H. *J. Chem. Soc., Chem. Commun.* **1982**, 640.

(22) See ref 17, Table 2.19.

and external ones have three each. The platinum atoms have no CO ligands. There are a total of 126 valence electrons. This can be rationalized as a combination of 84 electrons from the raft (as found in $Pt_3Fe_3(CO)_{15}$) plus 42 (3 × 14) from the three external ruthenium atoms.[18] When solutions of **4** in hexane solvent were heated to reflux, compound **5** was obtained in 37% yield by loss of all six hydride ligands and one of the CO ligands.

It is well-known that mercury is a poison for most hetergeneous catalytic reactions. In fact, mercury additions have been used as a test for heterogeneity in hydrogenation catalysis.[16] Accordingly, to test for the possible existence of heterogeneous processes in the catalysis produced by **1a**, we also conducted the hydrogenation reaction in the presence of mercury metal. There was no detectable decrease in catalytic activity of **1a** in the presence mercury, thus indicating the absence of heterogeneous catalytic hydrogenation processes.

To rule out the importance of catalysis by the platinum/ruthenium complexes that we isolated from the reaction, compounds **3a**, **4**, and **5** were independently tested for their catalytic activity. The TOFs for the hydrogenation of PhC_2Ph to (*Z*)-stilbene by **3a**, **4**, and **5** were 3.0, 1.8, and 0.6 h^{-1}, respectively. Although all showed some activity for this reaction, the activities are far too low to account for the bulk of the catalysis that is produced by the solutions of **1a**. In addition, a number of low nuclearity species that could have been formed by degradation of the **1a** were also tested. These included $Pt(PhC_2Ph)_2$,[7] $Ru_3(CO)_{12}$, $Ru(CO)_5$, and $Ru_3(CO)_9(\mu_3\text{-}PhC_2Ph)(\mu\text{-}H)_2$; the last of these has been reported previously to exhibit activity for the catalytic hydrogenation of PhC_2Ph.[9a] The TOFs for (*Z*)-stilbene formation exhibited by these complexes are 1.1, 2.2, 4.6, and 0.2 h^{-1}, respectively. For comparison, we also tested the related triruthenium and platinum diruthenium complexes $HRu_3(CO)_9(\mu_3\text{-ampy})(\mu\text{-H})$[10] and $PtRu_2(CO)_8(PhC_2Ph)(dppe)$.[11] Under our conditions, the TOFs for the formation of (*Z*)-stilbene by these compounds were 3.0 and 3.2 h^{-1}, respectively. It is also notable that, unlike **1a**, most of these compounds also produced significant quantities of (*E*)-stilbene (see Table 6).

Discussion

We have found that solutions of the compounds **1a,b** catalyze the selective hydrogenations of diphenylacetylene and ditolylacetylene to (*Z*)-stilbene and (*Z*)-ditolylethylene, respectively. Only small amounts of the *trans*-olefin and the fully hydrogenated species were detected. Several studies have described the catalytic hydrogenation of diphenylacetylene by metal cluster complexes recently, but none of these catalysts appear to be as active as the complexes **1a,b** reported here.[4b,9,10,16,23] The empirically derived rate equation (eq 1) was established. The nearly perfect linear dependence on the concentration of the cluster is indicative of a process that does not involve a fragmentation of the cluster.[24] There is both a first-order and inverse first-order dependence on alkyne concentration as revealed by the substantial intercept in the inverse plot, 1/rate vs $1/[PhC_2Ph]$, see Figure 3. There is a direct first-order dependence on the partial pressure of hydrogen, and an inverse first-order dependence on the partial pressure of CO was detected when CO was added to the system. The rate equation (eq 1) is similar to that reported for the catalytic hydrogenation of cyclohexene by $RhCl(PPh_3)_3$, which shows an inverse dependence on alkene and PPh_3 concentrations.[25]

Scheme 1

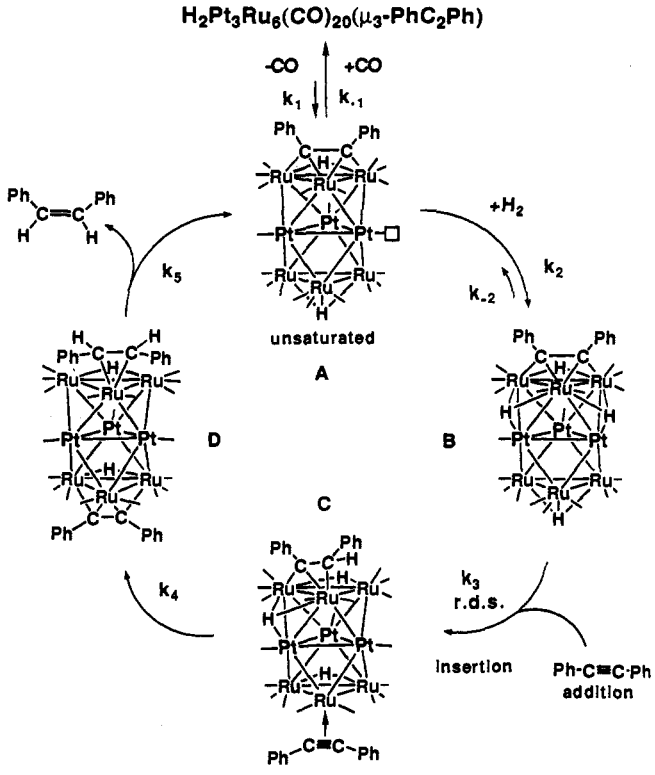

On the basis of this information, the mechanism for the catalysis shown in Scheme 1 is proposed. The inhibition by CO is interpreted in terms of an initial ligand dissociation step. This is reasonable because complex **1a** is formally electronically saturated and the activation of an additional hydrogen or alkyne would most likely proceed through the generation of a "vacant" coordination site provided by the dissociation of a ligand.[6,19] We have not been able to pinpoint experimentally the site of CO loss. However, it is suspected that the platinum may play some role in this for two reasons: (1) The complex $Ru_3(CO)_9(\mu_3\text{-}PhC_2Ph)(\mu\text{-}H)_2$, which has a close similarity to **1a** except for the absence of platinum, does not exhibit the high catalytic activity for the hydrogenation of PhC_2Ph that **1a** does. (2) It is known that CO ligands are not bonded as strongly to metals of the nickel subgroup as the they are to metals of the iron subgroup.[26] Accordingly, we have assigned the dissociation site to one of the platinum atoms, and the unsaturated intermediate **A** with a vacant site on one of the platinum atoms is the active catalyst. Intermediate **A** could react with hydrogen or alkyne. We have chosen hydrogen for the first step in reagent activation, but a competing formation of an alkyne adduct could occur at this stage and this could explain the inverse dependence of the catalysis on the alkyne concentration. We have also shown previously that **1a** will react with PhC_2Ph in the absence of hydrogen to yield **5**.[6a] We have allowed that the hydrogen activation step could be reversible, since treatment of **1a** with D_2 in the absence of alkyne showed the existence of a slow H/D exchange of the hydride ligands. The dissociation of CO from platinum is convenient to this hydrogen addition step, since platinum is known to have a great ability for hydrogen activation.[27] The hydrogen addition product **B** should be an electronically saturated complex with four hydride ligands. This species has not yet been observed, but in principle it could be. The distribution of the ligands shown in the figure is arbitrary, but

(23) (a) Cabeza, J. A.; Fernandez-Colinas, J. M.; Llamazares, A.; Riera, V. *Organometallics* **1993**, *12*, 4141. (b) Castiglioni, M.; Giordano, R.; Sappa, E. *J. Organomet. Chem.* **1989**, *369*, 419. (c) Castiglioni, M.; Giordano, R.; Sappa, E. *J. Organomet. Chem.* **1991**, *407*, 377.

(24) (a) Laine, R. M. *J. Mol. Catal.* **1982**, *14*, 137. (b) Hilal, H. S.; Jondi, W.; Khalaf, S.; Abu-Halawa, R. *J. Organomet. Chem.* **1993**, *452*, 161. (c) Hilal, H. S.; Khalaf, S.; Jondi, W. *J. Organomet. Chem.* **1993**, *452*, 167. (d) Sánchez-Delgado, R. A.; Andriollo, A.; Puga, J.; Martin, G. *Inorg. Chem.* **1987**, *26*, 1867. (e) Castiglioni, M.; Giordano, R.; Sappa, E. *J. Organomet. Chem.* **1989**, *362*, 399.

(25) (a) Osborn, J. A.; Jardine, F. H.; Young, J. F.; Wilkinson, G. *J. Chem. Soc. A* **1966**, 1711. (b) Halpern, J.; Wong, C. S. *J. Chem. Soc., Chem. Commun.* **1973**, 629. (c) Halpern, J.; Okamoto, T.; Zakhariev, A. *J. Mol. Catal.* **1976**, *2*, 65.

(26) (a) Lewis, K. E.; Golden, D. M.; Smith, G. P. *J. Am. Chem. Soc.* **1984**, *106*, 3905. (b) Stevens, A. E.; Feigerle, C. S.; Lineberger, W. C. *J. Am. Chem. Soc.* **1982**, *104*, 5026.

it is anticipated that the hydride ligands will prefer triply briding sites, such as have been observed in compound **3b**, see above. We anticipate that the next step is an alkyne addition to the saturated species **B** and may be the rate-determining step (rds). This is expected to occur without loss of a CO ligand since the CO inhibition appears to be only first order in CO pressure, and this was accounted for in the formation of **A**. We expect that the alkyne will add to one of the ruthenium triangles. We have no evidence to indicate which triangle at this time. In the scheme, we have shown addition to the non-alkyne-containing ruthenium triangle since an addition to the alkyne-containing triangle may be sterically more encumbered. The alkyne addition will increase the number of valence electrons in the cluster by two which should then exceed the normal valence count.[19] As a consequence, it is believed that the alkyne addition may simultaneously induce a transfer of one of the hydride ligands to the originally coordinated alkyne ligand, forming a C–H bond and converting the alkyne into an edge bridging 1,2-diphenylvinyl ligand with *cis*-positioned phenyl groups. This transformation will reduce the number of electrons in the cluster by two, thus the transformation of **B** to **C** will not result in a change in the electron count of the cluster. In support of this transformation, we have recently shown that **1a** will slowly add 1 equiv of CO to form the complex **7** (see above) that contains an edge bridging 1,2-diphenylvinyl ligand with *cis*-positioned phenyl groups.[6a] Alkyne ligands prefer to be bridging ligands in polynuclear metal complexes and serve as four electron donors;[28] therefore, it is expected that the alkyne ligand in **C** will readily shift into a triply bridging position similar to that found for the alkyne in **1a**. This shift would also increase the electron count at the cluster, and this could induce the shift of a hydride ligand to the edge bridging 1,2-diphenylvinyl ligand. This may lead to a species such as **D** that contains a coordinated (*Z*)-stilbene ligand. The steric bulk of the (*Z*)-stilbene ligand would favor its dissociation, which would regenerate the catalyst **A**. We anticipate that the **C** to **D** and **D** to **A** transformations will be kinetically fast and the alkyne addition/CH migration of **B** to **C** will represent the slow step. Migration of hydrogen to the alkene ligand was found to be the slow step in hydrogenation of olefins by Wilkinson's catalyst. Curiously, we have obtained no evidence for a measurable kinetic isotope effect on the rate of the reaction as might be expected if the hydrogen shift were the slow step. Interestingly, the deuterium isotope effect observed in the hydrogenation of olefins by Wilkinson's catalyst is very small.[25]

Using these assumptions and applying the steady state approximation to the concentration of the species **B**, it is possible to derive the rate expression (eq 2) based on the species **A** as the

$$\text{rate} = k_3[\text{B}][\text{alkyne}] = \frac{k_3k_2[\text{A}]p(\text{H}_2)[\text{PhC}_2\text{Ph}]}{(k_{-2} + k_3[\text{PhC}_2\text{Ph}])} \quad (2)$$

catalyst. k_2, k_{-2}, and k_3 are the specific rate constants as indicated in Scheme 1. If one substitutes a value for the concentration of **A** based on a CO dissociative equilibrium involving **1a**, then expression 3 emerges, which is formally equivalent to the empirical expression (eq 1). K_1 is the equilibrium constant for the dissociation of CO, k_1/k_{-1}.

$$\text{rate} = k_3[\text{B}][\text{PhC}_2\text{Ph}] = \frac{K_1k_3k_2[1\text{a}]p(\text{H}_2)[\text{PhC}_2\text{Ph}]}{p(\text{CO})(k_{-2} + k_3[\text{PhC}_2\text{Ph}])} \quad (3)$$

Probably the strongest evidence that **1a** is tied directly to the catalysis was derived from the tracer studies, the hydrogenation of ditolylacetylene by **1a**, and the deuteration of ditolylacetylene by **1b**. These tests were made possible by the fact that **1a** contains both reagents of the catalytic reaction, hydrogen and the alkyne, as ligands. If **1a** is tied directly to the catalytic species, then the reagents must enter into binding with it and replacement of the ligands with the reagents can be anticipated. *Indeed this was observed in both tests.* Notably, this exchange either did not occur or was minimal when the actual catalytic process was not in progress (i.e., the control experiments). Conversely, a negative result would have strongly suggested that **1a** was not tied directly to the catalytic process.

Other negative tests such as the mercury test for heterogeneous catalysis and investigation of low-nuclearity species that might have resembled fragment species produced by degradation of the cluster provide indirect support that **1a** is tied directly to the catalytic process. In addition, it was shown by the 1000/1 PhC_2-Ph/**1a** experiment that, when **1a** was degraded, the catalytic activity declined, contrary to what might be expected if the degradation was actually producing the catalytically active fragments.

Some interesting high-nuclearity platinum–ruthenium cluster complexes were isolated from the catalytic mixtures, **2a**, **3a**, **3b**, **4**, and **5**. Clearly, these were derived from the reactions of **1a** with the hydrogen and/or the PhC_2Ph, but independent tests of the catalytic activity of these compounds rule them out as the species responsible for the bulk of the catalysis.

The temperature-dependent studies have revealed activation parameters, $\Delta H^* = 24.9(6)$ kcal/mol and $\Delta S^* = 1.4(9)$ eu, that are higher than, but not vastly different from, those of Wilkinson's famous catalyst for the hydrogenation of cyclohexene, $\Delta H^* = 22.3$ kcal/mol and $\Delta S^* = 12.9$ eu.[25a]

The most important results of this study are (1) the presentation of convincing evidence that the high-nuclearity layer-segregated platinum–ruthenium cluster complex **1a** is directly tied to a highly selective process for the catalytic hydrogenation of PhC_2Ph to (*Z*)-stilbene at an unusually high level of activity and (2) the demonstration that a complex of two different types of metals, platinum and ruthenium, leads to a catalyst that is superior to those derived from complexes of the elements when separated. We suspect that this synergism may result from a bifunctional character of the catalyst, in particular, the platinum atoms activate the hydrogen and the ruthenium atoms activate the alkyne, although future studies will be needed to establish further details of the mechanism.

Synergism has also been observed by mixed metal heterogeneous catalysts,[29] and studies have shown that platinum–ruthenium bimetallic particles exhibit catalytic properties for hydrogenation[30] and alkane isomerizations that are superior to those of the separated metals.[31]

Acknowledgment. These studies were supported by the National Science Foundation under Grant No. CHE-9224141. We wish to thank Professor Robert G. Bergman for helpful suggestions.

Supplementary Material Available: Tables of atomic positional parameters and anisotropic thermal parameters for each of the structural analyses (22 pages); tables of structure factors (68 pages). This material is contained in many libraries on microfiche, immediately follows this article in the microfilm version of the journal, and can be ordered from the ACS; see any current masthead page for ordering information.

(27) Bond, G. C. In *Catalysis by Metals*; Academic Press: London, 1962; Chapter 8.

(28) (a) Raithby, P. R.; Rosales, M. J. *Adv. Inorg. Radiochem.* **1985**, *29*, 169. (b) Sappa, E.; Tiripicchio, A.; Braunstein, P. *Chem. Rev.* **1983**, *83*, 203.

(29) Rylander, P. N. In *Catalytic Hydrogenation over Platinum Metals*; Academic Press: New York, 1967; Chapter 1.

(30) (a) Diaz, G.; Garin, F.; Maire, G. *J. Catal.* **1983**, *82*, 13. (b) Gomez, R.; Corro, G.; Diaz, G.; Maubert, A.; Figueras, F. *Nouv. J. Chem.* **1980**, *4*, 677. (c) Maetz, P.; Diaz Guerrero, G.; Touroude, R. *React. Kinet. Catal. Lett.*, in press.

(31) Gray, T. J.; Masse, N. G.; Oswin, H. G. *Proc. Int. Congr. Catal., 2nd* **1961**, 1697.